Arch. Metall. Mater., Vol. 61 (2016), No 3, p. 1441–1446

DOI: 10.1515/amm-2016-0236

K. OSIŃSKA*,#, M. PŁOŃSKA*, A. MARZEC**

APPLICATION OF THE SOL-GEL METHOD AT THE FABRICATION OF PLZT:Yb^{3+} CERAMICS

The aim of presented study was to obtain the PLZT:Yb^{3+} ceramics. Nanopowders of itterbium doped PLZT materials were synthesized by the sol-gel method from high quality metaloorganic precursors, as lead (II) acetate, lanthanum acetate, ytterbium acetate, zirconium (IV) propoxide and titanium (IV) propoxide. Anhydrous acetic acid and n-propyl alcohol were used as solvents, while acetyloacetone was added as stabilizer of hydrolysis reactions. Thermal evolution of the dried gels, before and after calcination, was studied by the simultaneous thermal analysis. The amorphous PLZT:Yb^{3+} gels were first calcined in the furnace at T = 850°C, and then mixed in the planetary ball mill. Additionally, the mean particle sizes were calculated by means of powder specific surface area measurements, based on the BET physical adsorption isotherm. Such obtained powders were subsequently pressed into pellets, and sintered by the free sintering method at temperature T = 1250°C / 6h. The morphology of fabricated PLZT:Yb^{3+} ceramic powders and samples was studied using Scanning Electron Microscopy. Chemical characterization of samples was carried on using the Energy-dispersive X-ray spectroscopy - EDS system. Studies provided detailed data concerning the relationships between doping and preparing conditions on the basic physical and chemical properties of obtained ceramic materials.

Keywords: PLZT:Yb^{3+} ceramics, sol-gel method, perovskite structure ceramics

1. Introduction

Lead zirconate titanate $Pb(Zr_{1-x}Ti_x)O_3$ (PZT) is one of the world's most widely used piezoelectric ceramic material. The PZT material has a perovskite type crystal structure, where each unit consists of a small tetravalent metal ion, in a lattice of large divalent metal ions. In the case of PZT ceramics, the small tetravalent metal ion is usually titanium or zirconium, when the large divalent metal ion is usually lead. Provided that, it confers a tetragonal or rhombohedral symmetry on the PZT crystals, and each of them has a dipole moment [1, 2].

It is accepted that the lanthanum addition causes a distortion in the unit cell of PZT system. In a consequence it reduces the optical anisotropy in the crystalline lattice, and leads to a growth of uniform grains with only one dense phase, as well promotes a free porous structure [3]. The doping of La^{3+} ions to the basic PZT system results in many beneficial effects such as increased squareness of the P–E hysteresis loops, decreased coercive field (Ec), enhanced dielectric and piezoelectric properties and large electromechanical coupling coefficients, improved mechanical compliance and transparency [4]. As a result, the PLZT ceramic materials have been widely used over recent decades for optical sensor and actuator devices. The PLZT powders were prepared using various methods: by a solid-state reaction process using oxides as starting materials [5], by a sol-gel method [6], by chemical coprecipitation [7], by hydrothermal reaction [8], by molten salt synthesis [9] and by a high-energy ball milling process [10].

In an attempt to get improved properties, ceramics is subjected to co-doping with diamagnetic ions as well as rare-earth cations. Substitution of the rare-earth cations (RE^{3+}) can effectively modulate the crystal structure parameters and change luminescence properties of based PLZT ceramics [11]. Recently, the PLZT:RE^{3+} ceramics are promising modified materials, which can be used as some electro-optical elements, optical sources and amplifiers or multifunction compact devices [12].

In this paper, the conditions of preparation of ytterbium doped 8/65/35 PLZT nanopowders (8/65/35 PLZT:Yb^{3+}) using the sol-gel method has been presented. The relationship between the amount of Yb^{3+} dopant in composition of 8/65/35 PLZT ceramics and their physical and chemical properties has been also discussed.

2. Experimental

Nanopowders of ytterbium doped $(Pb_{0.92}La_{0.08})(Zr_{0.65}Ti_{0.35})_{0.98}O_3$ (8/65/35 PLZT) materials were synthesized via the sol-gel method. Lead (II) acetate, lanthanum acetate, zirconium (IV) propoxide and titanium (IV) propoxide were used as starting materials of the basic 8/65/35 PLZT ceramics. The ytterbium acetate dopant was added in weight percent for c_w = 0, 0.5%, 1.5%, 2.5% (8/65/35 PLZT:$Yb^{3+}c_w$). As solvent for lead (II) acetate, and lanthanum acetate an anhydrous acetic acid was used. After dissolving both precursors at T = 100°C for t = 0.5 h, the mixture was cooled down to a room temperature.

---

* UNIVERSITY OF SILESIA, INSTITUTE OF TECHNOLOGY AND MECHATRONICS, 2, SNIEZNA STR., SOSNOWIEC, 41-200 POLAND

** UNIVERSITY OF SCIENCE AND TECHNOLOGY, FACULTY OF MATERIALS SCIENCE AND CERAMICS, DEPARTMENT OF CERAMICS AND REFRACTORY MATERIALS, AL. MICKIEWICZA 30, 30-059 KRAKOW, POLAND

Corresponding author: katarzyna.osinska@us.edu.pl

After mixing zirconium (IV) propoxide and titanium (IV) propoxide in n-propyl alcohol, Pb-La-Yb solution was mixed with Zr-Ti solution by magnetic stirrer for t = 1 h. Then the solution was hydrolyzed by adding of distilled water. Subsequently a small amount of acetyloacetone was added as stabilizer of solution system. The resulting sol was relatively stable and became a gel in a few days. The amorphous 8/65/35 PLZT:Yb$^{3+}c_w$ gels were dried and later calcined in the furnace at T = 850°C for t = 4 h. After calcinations the obtained powders were wet milled in the planetary ball mill, for t = 24 h respectively for each composition using YTZ balls as grinding media (of 2/5 mm in diameter) in ethanol solution. Then it was pressed into pellets of d = 10 mm diameter and h = 2 mm thick at p = 600 MPa. The compacts were subsequently sintered by the free sintering method at temperature T = 1250°C for t = 6 h.

The dry samples of gels 8/65/35 PLZT:Yb^{3+}cw, before and after calcination, were analyzed by the Thermo-Gravimetric Analysis (TGA) as well by the Differential Thermal Analysis (DTA). Simultaneous measurements were performed in air, using a derivatograph of Q-1500D- type (Paulik-Paulik-Erdey system), for prepared compositions samples about mass $m \sim 50$ mg of each.

The mean particle sizes were calculated by means of powder specific surface area measurements, based on the BET physical adsorption isotherm. The measurements were performed on a NOVA 1200e analyzer by Quantachrome Instruments with nitrogen as the adsorbate. The mean particle sizes of the powders were estimated based on the values of specific surface areas using correlation:

$$D_{BET} = \frac{6000}{d \cdot S_w}, \tag{1}$$

where: D_{BET} – estimated particle size [nm], d – density of the material [g/m^3], S_w – specific surface area of the powder, measured using the BET physical adsorption isotherm [m^2/g].

The apparent density of the sintered 8/65/35 PLZT:Yb^{3+}cw ceramic samples was measured by the Archimedes method, while the morphology of synthesized ceramic powders and fracture surface of sintered ceramics were studied by Scanning Electron Microscope (type HITACHI S-4700). The stoichiometry of obtained ceramics was investigated using EDS-NORAN Vantage system of microanalysis.

3. Results and discussion

At Figures 1 (a - d), have been shown thermal analysis curves of dry gels of the 8/65/35 PLZT: Yb^{3+} c_w before calcinations. One can see all dried gels were exhibited a large total weight loss $\Delta m \approx 40\%$ for 8/65/35 PLZT:Yb^{3+}0, $\Delta m \approx 40\%$ for 8/65/35 PLZT:Yb^{3+}0.5, $\Delta m \approx 43\%$ for 8/65/35 PLZT:Yb^{3+}1.5, and $\Delta m \approx 46\%$ for 8/65/35 PLZT:Yb^{3+}2.5, respectively. The analysis has shown three stages of weight loss. The peak on the DTG curve at

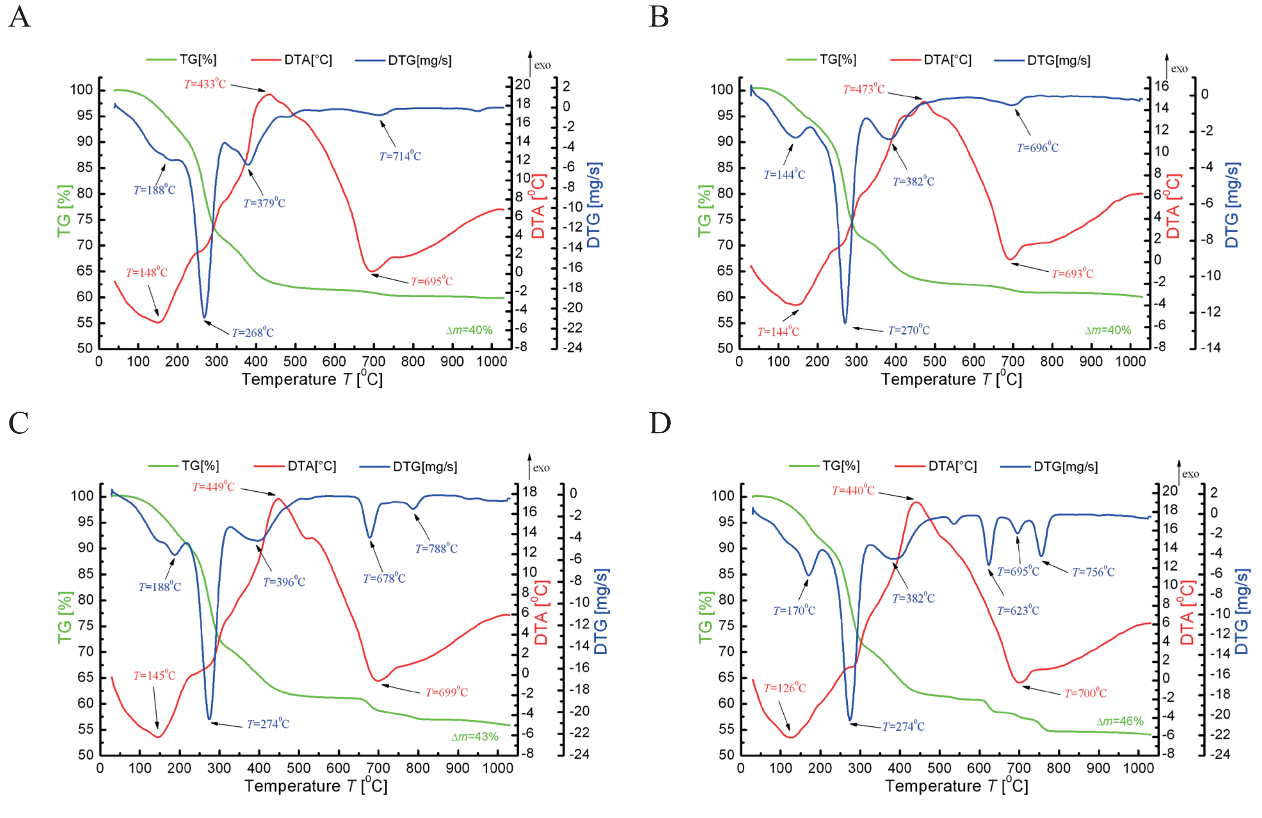

Fig. 1. Thermal analysis data of the 8/65/35 PLZT:Yb$^{3+}c_w$ dry gels before calcinations, where: (A) c_w = 0 wt.%; (B) c_w = 0.5 wt.%; (C) c_w = 1.5 wt.%; (D) c_w = 2.5 wt.%

around T = 188°C and corresponding weight loss $\Delta m_1 \approx 10\%$ for 8/65/35 PLZT:Yb^{3+}0 on the TG curve, T = 144°C and corresponding weight loss $\Delta m_1 \approx 10\%$ for 8/65/35 PLZT:Yb^{3+}0.5 on the TG curve, T = 188°C and corresponding weight loss $\Delta m_1 \approx 10\%$ for 8/65/35 PLZT:Yb^{3+}1.5 on the TG curve, T = 170°C and corresponding weight loss $\Delta m_1 \approx 10\%$ for 8/65/35 PLZT:Yb^{3+}2.5 on the TG curve are the result of evaporation of the solvents. The endothermic maxima on DTA curves accompany peaks on DTG curves.

The second notable weight loss $\Delta m_2 \approx 27\%$ was detected at T = 268°C and T = 379°C for 8/65/35 PLZT:Yb^{3+}0, $\Delta m_2 \approx 27\%$ was detected at T = 270°C and T = 382°C for 8/65/35 PLZT:Yb^{3+}0.5, $\Delta m_2 \approx 27\%$ was detected at T = 274°C and T = 396°C for 8/65/35 PLZT:Yb^{3+}1.5, $\Delta m_2 \approx 30\%$ was detected at T = 274°C and T = 382°C for 8/65/35 PLZT:Yb^{3+}2.5. They correspond to the large exothermic peaks on the DTA curve (T = 433°C, T = 473°C, T = 449°C, T = 440°C, respectively). Crystallization didn't take place below T = 500°C, so the weight loss was probably due to the decomposition of organic additives in the gel.

The third notable drop between $T \approx$ 600°C and $T \approx$ 8500C, corresponds to the peaks on the DTG curve at about T = 714°C for 8/65/35 PLZT:Yb^{3+}0, T = 696°C for 8/65/35 PLZT:Yb^{3+}0.5, T = 678°C and T = 714°C for 8/65/35 PLZT:Yb^{3+}1.5 as well as T = 623°C, T = 695°C and T = 756°C for 8/65/35 PLZT:Yb^{3+}2.5. The third weight loss ($\Delta m_3 \approx 3\%$ for 8/65/35 PLZT:Yb^{3+}0, $\Delta m_3 \approx 3\%$ for 8/65/35 PLZT:Yb^{3+}0.5, $\Delta m_3 \approx 6\%$ for 8/65/35 PLZT:Yb^{3+}1.5, $\Delta m_3 \approx 6\%$ for 8/65/35 PLZT:Yb^{3+}2.5) originates from the release of various side products during alcoxolation and oxolation. The endothermic maxima on DTA

TABLE 1

The weight loss values and characteristic temperatures of TG/DTG/DTA analysis for 8/65/35 PLZT:Yb$^{3+}c_w$ dry gel after calcinations

Composition of 8/65/35 PLZT:Yb$^{3+}c_w$	Yb$^{3+}c_w$			
	0 wt.%	0.5 wt.%	1.5 wt.%	2.5 wt.%
Total weight loss values Δm [%]	3	4	5	6
Temperature on DTG for first weight loss T [°C]	123, 254, 344	124, 251, 351, 446	131, 253, 353, 427	130, 258, 356, 439
Temperature on DTG for second weight loss T [°C]	714	672	679	688
Temperature on DTA for endothermic changes T [°C]	122, 274, 432, 797	113, 276, 491, 847	122, 269, 370, 503, 738	120, 274, 371, 500, 759
Temperature on DTA for exothermic changes T [°C]	232, 329, 505	225, 328, 396, 534	221, 328, 404, 557	227, 320, 416, 570, 809

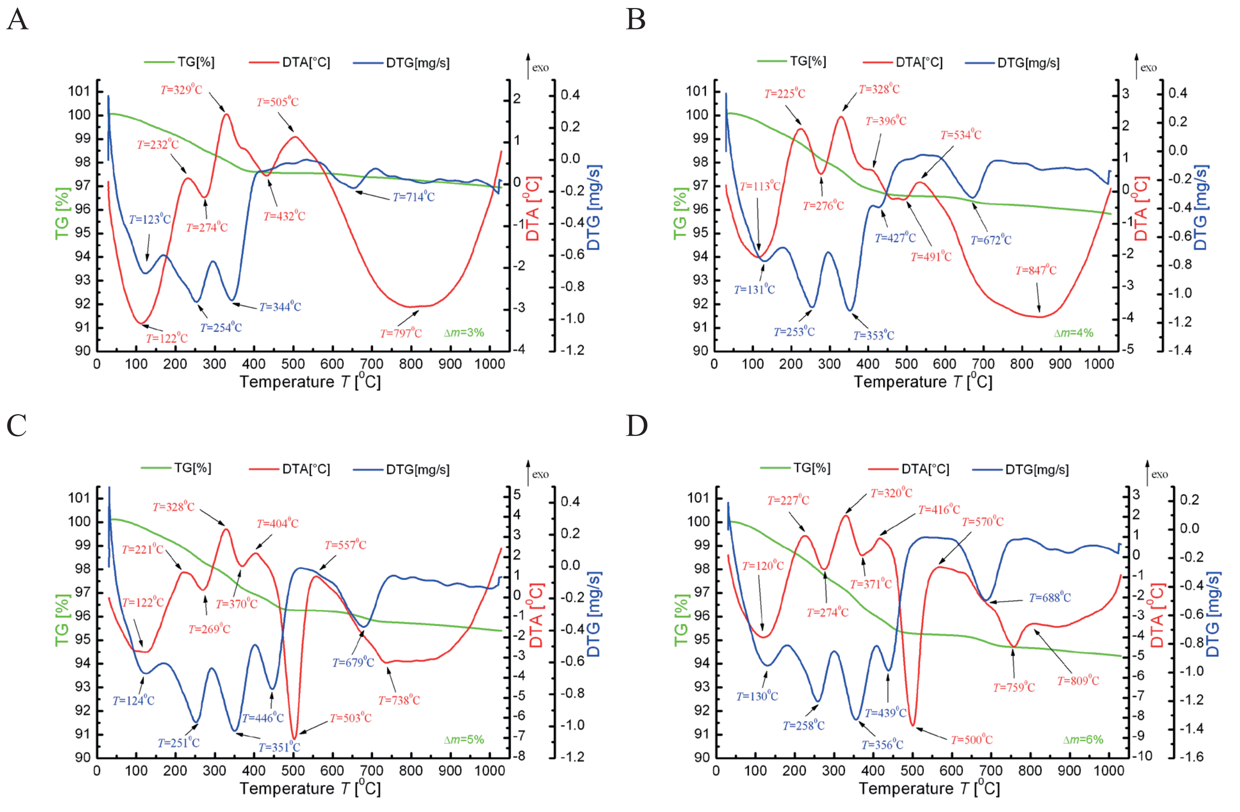

Fig. 2. Thermal analysis data of the 8/65/35 PLZT:Yb$^{3+}c_w$ dry gels after calcinations, where: (A) c_w= 0 wt.%; (B) c_w = 0.5 wt.%; (C) c_w = 1.5 wt.%; (D) c_w = 2.5 wt.%

curves at $T = 695°C$, $T = 693°C$, $T = 699°C$ and $T = 700°C$ for successive compositions, were the results of transformation of the amorphous phase into the perovskite phase.

On the basis of thermal analysis, the calcination temperature $T = 850°C$ was chosen for all dried gels.

Thermal analysis curves of the dry gels after calcinations were shown at Figures 2a, 2b, 2c and 2d, respectively. The weight loss values and characteristic temperatures of TG/DTG/DTA analysis for 8/65/35 PLZT:Yb$^{3+}c_w$ dry gel after calcinations are given in TABLE 1. The first weight loss occurs in a temperature range $\Delta T = 50$ - 500°C and the second weight loss occurs in a temperature range $\Delta T = 500$ - 900 °C for all compositions of the 8/65/35 PLZT:Yb$^{3+}c_w$ materials.

Figures 2a, 2b, 2c and 2d have shown that after calcination no large thermal effects, which take place with powdered gels before calcinations, occured.

In case of the nanocrystalline powders, the most important parameters characterizing the material are phase composition and the grains size. The obtained powders of 8/65/35 PLZT:Yb$^{3+}c_w$ were characterized by a significantly expanded specific surface area. Values of specific surface area (S_w) of the powder measured using the BET physical adsorption isotherm [m^2/g], and estimated particle size D_{BET} are shown in TABLE 2.

TABLE 2

Specific surface area measured using the BET physical adsorption isotherm S_w and estimated particle size D_{BET} of the 8/65/35 PLZT:Yb$^{3+}c_w$ powders

Composition of 8/65/35 PLZT:Yb$^{3+}c_w$ Where c_w [wt.%]	S_w [m^2/g]	D_{BET} [nm]
0	11.32	66.25
0.5	11.12	67.45
1.5	12.51	59.95
2.5	16.02	46.82

Density of samples was measured by the Archimedes' method and the apparent density of the 8/65/35 PLZT:Yb$^{3+}c_w$ ceramics samples was found $\rho = 7$ g/cm^3, approximately.

Scanning electron micrographs and analysis of EDS spectrum of the sintered 8/65/35 PLZT:Yb$^{3+}c_w$ ceramic samples are given in Figures 3a, 3b, 3c and 3d, respectively.

It is well known that preparing of the fully dense nanostructure ceramics it is difficult process, due to a lot of factors, which can affect on producing fine-grained materials with high density. The powders synthesis process, sintering temperature as well dwell time has the strong influence on the

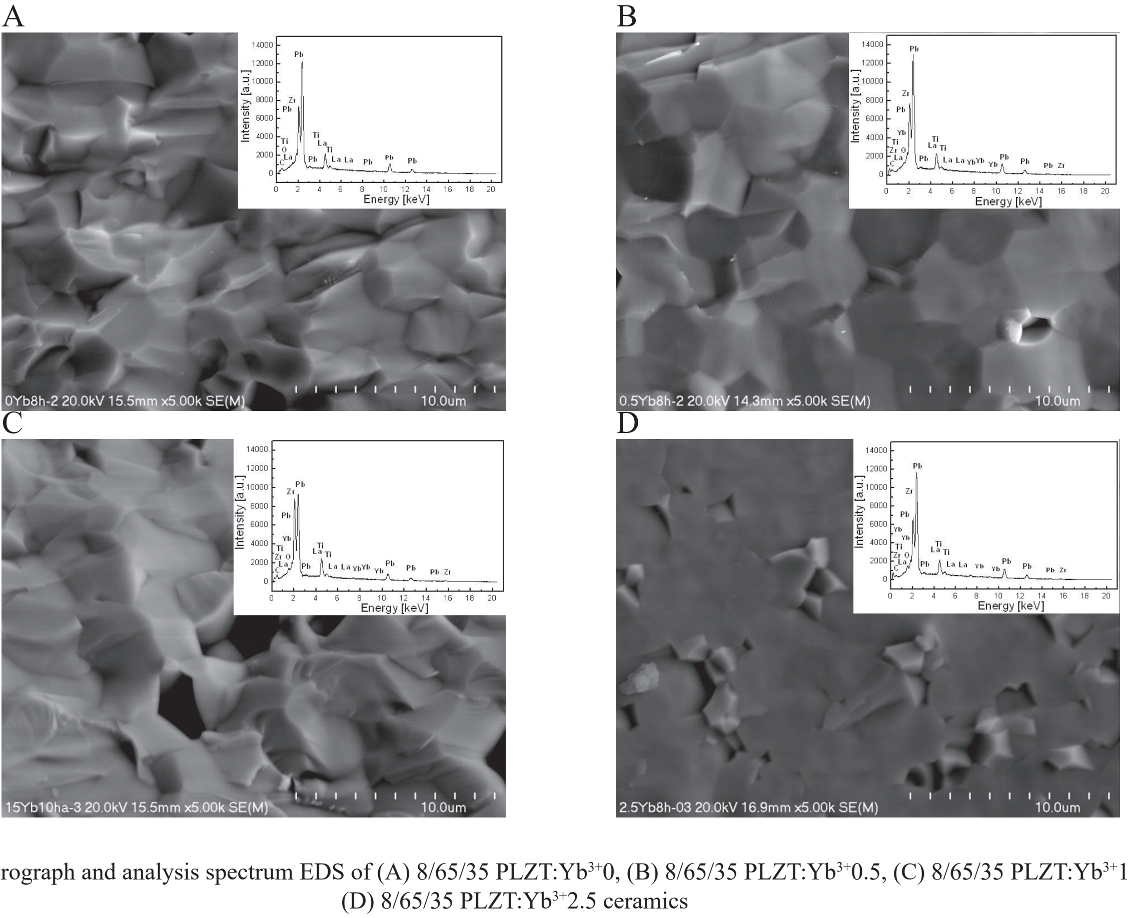

Fig. 3. SEM micrograph and analysis spectrum EDS of (A) 8/65/35 PLZT:Yb^{3+}0, (B) 8/65/35 PLZT:Yb^{3+}0.5, (C) 8/65/35 PLZT:Yb^{3+}1.5 and (D) 8/65/35 PLZT:Yb^{3+}2.5 ceramics

TABLE 3

Theoretical and determined chemical composition of 8/65/35 PLZT:Yb$^{3+}c_w$

Sample with Yb$^{3+}c_w$ [wt.%]	Theoretical compositions of the 8/65/35 PLZT:Yb$^{3+}c_w$ in the count on oxides [wt.%]					Determined compositions of the 8/65/35 PLZT:Yb$^{3+}c_w$ in the count on oxides [wt.%]				
	%PbO	%La$_2$O$_3$	%ZrO$_2$	%TiO$_2$	%Yb$_2$O$_3$	%PbO	%La$_2$O$_3$	%ZrO$_2$	%TiO$_2$	%Yb$_2$O$_3$
0	63.32	4.02	24.21	8.45	---	62.29	3.88	24.98	8.85	---
0.5	62.96	4.00	24.07	8.40	0.57	61.43	3.84	25.43	8.69	0.61
1.5	62.25	3.95	23.80	8.30	1.70	61.92	3.77	24.79	8.04	1.48
2.5	61.53	3.90	23.52	8.21	2.84	60.25	3.69	25.39	8.15	2.52

powders agglomeration. In case of prepared samples, it was observed that the shape of the powder particles was not uniform and angular grains had sharp edges. Samples of the obtained materials were compact, homogeneous and non-porous. The grain sizes of the 8/65/35 PLZT:Yb$^{3+}c_w$ ceramics seems to be similar in all samples, although it can be noted that ytterbium concentration has slight influence on their size.

In the Table 3, the values of the theoretical and measured chemical compositions are presented. Results for each of the investigated samples have been presented in wt.%, as the count on oxides.

One can see the 8/65/35 PLZT:Yb$^{3+}c_w$ ceramics, fabricated according to presented technology, exhibited stoichiometric composition with an accuracy typical for the measuring method applied. Results of EDS analysis for all ceramic samples are very close to the theoretical stoichiometric ratio in each of prepared composition, and confirm a high purity and homogeneity of the obtained materials. Probably the 6 hours of the sintering process might increase the volatility loss of lead oxide that serves as a source of point vacancies in the volumetric structure of the materials.

4. Conclusions

The sol gel method was successfully utilized for synthesis of the 8/65/35 PLZT:Yb$^{3+}c_w$ ceramic powders. On the basis of thermal analysis, the temperature of calcinations was chosen T = 850°C for all dried gels. The obtained nanopowders were characterized by significant expansion of the specific surface area, and it was observed decreasing of particle size with the increasing of ytterbium dopant amount. The 8/65/35 PLZT:Yb$^{3+}c_w$ ceramic samples were finally sintered at temperature T = 1250°C for t = 6h. Ceramics samples of 8/65/35 PLZT:Yb$^{3+}c_w$ were compact, homogeneous and non-porous. Results of EDS analysis for all ceramic samples were very close to the theoretical stoichiometric ratio in each of prepared composition, and confirmed a high purity and homogeneity of obtained materials.

Acknowledgments:

The present research has been supported by National Science Centre in years 2013-2017, as a research project No UMO-2012/07/D/ST8/02634.

REFERENCES

[1] J. Jurczyk, B. Zawisza, R. Sitko, F. Buhl, K. Osińska, M. Płońska, Chem. Anal. **47**, 925 -934 (2002).
[2] E. Nogas-Cwikiel, Arch. Metall. Materials. **56**, 1065 - 1069 (2011).
[3] M. Cerqueira, R.S. Nasar, E.R. Leite, E. Longo, J.A. Varela, Sintering and characterization of PLZT (9/65/35), Ceram. Int. **26**, 231 - 236 (2000).
[4] L. B Kong, J Ma, W Zhu, O. K Tan, J. Alloy Compd **322**, 290 - 297 (2001).
[5] P. Wawrzała, J. Korzekwa, Ferroelectrics **446**, 91 - 101 (2013).
[6] M. Płońska, W. A. Pisarski, Z. Pędzich, Z. Surowiak, Advances in Science and Technology **45**, 2489 - 2494 (2006).
[7] R. Gunawidjaja, T. Myint, H. Eilers, Ceram. Int. **38**, 775 - 786 (2012).
[8] R. Zhu, K. Zhu, J. Qiu, Y. Zheng, H. Ji, Kuei Suan Jen Hsueh Pao/Journal of the Chinese Ceramic Society **38**, 627 (2010).
[9] Z. Cai, X. Xing, L. Li, J. Alloy Compd. **454**, 466 - 470 (2008).
[10] A.R. James, BS. S.C. Rao, S.V. Kamat, J. Subrahmanyam, K. Srinivas, O.P. Thakur, VTT SYMP **17**, 035020 (2008).
[11] J. Dzik, H. Bernard, K. Osińska, A. Lisińska-Czekaj, D. Czekaj, Arch. Metall. Materials. **56**, 1119 (2011).
[12] M. Płońska, W.A. Pisarski, B. Wodecka-Duś, D. Czekaj, Arch. Metall. Materials. **58**, 1365 - 1369 (2013).